Current Research in Food Science 5 (2022) 687–697

Contents lists available at ScienceDirect

Current Research in Food Science

journal homepage: www.sciencedirect.com/journal/current-research-in-food-science

Research Paper

Formulations with microencapsulated Fe–peptides improve *in vitro* bioaccessibility and bioavailability

Bruna Gaigher [a], Emanueli do Nascimento da Silva [b,c], Vitor Lacerda Sanches [c], Raquel Fernanda Milani [a], Fabiana Galland [a], Solange Cadore [c], Mariana Grancieri [d], Maria Teresa Bertoldo Pacheco [a,*]

[a] Institute of Food Technology (ITAL), Brasil Avenue 2880, PO Box 139, 13070-178, Campinas, SP, Brazil
[b] Department of Chemistry, Institute of Exact and Biological Sciences, Federal University of Ouro Preto, Ouro Preto, MG, Brazil
[c] Institute of Chemistry, University of Campinas, Campinas, SP, Brazil
[d] Department of Nutrition and Health, Federal University of Viçosa, Viçosa, MG, Brazil

ARTICLE INFO

Keywords:
Iron-peptide
Microencapsulated active
Bioaccessibility
Caco-2 cells
Dialyzability
Molecular coupling

ABSTRACT

The bioaccessibility and the bioavailability of iron complexed to peptides (active) in microparticles forms contained in dry beverages formulations were evaluated. The peptide-iron complexes microparticles were obtained by spray drying and added in three dry formulations (tangerine, strawberry, and chocolate flavors). The peptides isolated by iron ion affinity (IMAC-Fe III) had their biological activity predicted by BIOPEP® database and were evaluated by molecular coupling. The bioaccessibility was evaluated by solubility and dialysability and the bioavalability was assessed by Caco-2 cellular model. The proportion 10:1 of peptide-iron complexes presented higher rates of bioaccessibility (49%) and bioavailability (56%). The microparticle with peptide-iron complex showed greater solubility after digestion (39.1%), bioaccessibility (19.8%), and bioavailability (34.8%) than the ferrous sulfate salt (control) for the three assays (10.2%; 12.9%; 9.7%, respectively). Tangerine and strawberry formulations contributed to the iron absorption according to the results of bioaccessibility (36.2%, 30.0% respectively) and bioavailability (80.5%, 84.1%, respectively). The results showed that iron peptide complexation and microencapsulation process improve the bioaccessibility and bioavailability when incorporated into formulations.

1. Introduction

Food fortification refers to the addition of trace elements and vitamins to food products. The fortification of food requires a suitable food vehicle, commonly consumed by the population to get high bioavailability of nutrients (Hurrell and Egli, 2019). This practice aims to improve its nutritional quality and at the same time provide some benefit, with a minimum risk to the health of the population (WHO, 2016). Although fortification is considered relatively simple to prevent mineral deficiency and adopted in many countries, it is still a major challenge for the food industry (Hurrell, 2002). In relation to iron, the difficulties are related to the bioavailability of this mineral, oxidative stability, and also sensory changes in food (Blanco-Rojo and Vaquero, 2019; Caetano-Silva et al., 2017; Gharibzahedi and Jafari, 2017; Shubham et al., 2020).

Iron peptides complexes may represent a potential alternative for chemical iron fortification of food products (Athira et al., 2021). However, many interactions within food complexes fortification and digestion process may compromise the bioaccessibility and bioavailability of the metal. The bioaccessibility represents the proportion of mineral available for absorption after digestion process. Moreover, bioavailability is represented by the proportion of ingested metal available for metabolic process or stored (Blanco-Rojo and Vaquero, 2019). Therefore, the evaluation of bioaccessibility and available absorption of iron may represent an important factor for the development of news formulations.

Iron deficiency compromises the physical and mental development of children with impaired learning ability with reflexes in adulthood, where they manifest a reduction in the physical work capacity and productivity of manual tasks (Antunes and Canziani, 2016; Ren et al.,

* Corresponding author.
E-mail address: mtb@ital.sp.gov.br (M.T. Bertoldo Pacheco).

https://doi.org/10.1016/j.crfs.2022.03.007
Received 26 November 2021; Received in revised form 4 March 2022; Accepted 17 March 2022
Available online 24 March 2022

2011; Szarfarc, 2010; Zhang et al., 2014). The costs generated by iron deficiency anemia due to loss of physical productivity have been estimated at around 0.81% of gross domestic product in low and middle-income countries (WHO, 2016). Given that 800 million children and women are affected by anemia, its reduction has become a priority target for global nutrition projected for 2025 by the World Health Organization (WHO, 2016).

Iron, when ingested in the form of salt, has low bioavailability, might promote the formation of reactive oxygen species (ROS) and irritations in the gastric mucosa (Abdel Moety et al., 2017). Organic compounds, such as proteins and peptides, have been shown to increase iron up-take on Caco-2 cell line model. Particularly, peptides generated from whey proteins have been identified as efficient iron chelators (Argyri et al., 2009; Etcheverry et al., 2012; Lv et al., 2014; Ou et al., 2010; Xu et al., 2017). The complexation of iron with organic compounds prior to ingestion may represent a good strategy to reduce iron-lipid peroxidation (Guzun-Cojocaru et al., 2011; Sugiarto et al., 2010), increase solubility (Ueno et al., 2014) and bioavailability (Caetano-Silva et al., 2018; Eckert et al., 2016; Wang et al., 2014; Zhu et al., 2009). Therefore, it is a promising ingredient in the elaboration of mineral supplements, for use in the treatment of iron deficiency anemia (Athira et al., 2021; Caetano-silva, Bertoldo-pacheco, Paes-leme, & Maria, 2015; Caetano--Silva et al., 2018; Hoz et al., 2014; Zhou et al., 2012).

There are still few studies that evaluate bioaccessibility and estimate the bioavailability of Fe-peptide complexes, obtained from whey protein hydrolysates, and even more scarce are studies evaluating these complexes in food matrices (Caetano-Silva et al., 2018; Sun et al., 2020). Thus, based on the conditions that our group have been studied to obtain iron-peptide complexes, the present work aimed to evaluate the bioaccessibility (by dializability and *in vitro* gastrointestinal simulation) and estimate the *in vitro* bioavailability of iron present in dry beverage formulations, containing microparticles as carriers of Fe-peptide complexes.

2. Material e methods

2.1. Reagents and materials

Whey protein isolate (WPI) was kindly provided from Fonterra Cooperative Group Limited (Auckland City, New Zealand) and the enzyme Alcalase® (Bacillus licheniformis, activity 2.4 μg-1 protein) from Novozymes Latin America Ltda. (Araucária, PR, Brazil). Ferrous sulfate ($FeSO_4$/12353) and enzymes (amylase/86250, pepsin/p7000, pancreatin/P1625, bile/B8631) were purchased from Sigma-Aldrich (St. Louis, MO, USA). Caco-2 cells (passage 45) were purchased from Banco de Células do Rio de Janeiro (BCRJ, Rio de Janeiro, Brazil).

2.2. Enzymatic hydrolysis of whey isolate and fractionation

The whey protein isolate was diluted in water (10% w/v) and the enzyme Alcalase® was added under conditions determined in previous studies (pH 8.0, 1:1 enzyme/substrate ratio at 60 °C, 180 min). In sequence, the total hydrolyzate was fractionated in a Pellicon® ultrafiltration system (Millipore, Bedford, MA, USA) with a 5 kDa molecular cut membrane and, only the retained fraction (<5 KDa) was used for synthesis of peptides-iron complexes. Degree of hydrolysis (DH) was determined by the o-phthaldialdehyde (OPA) method, as described by Nielsen et al. (2001).

2.3. Amino acid profile of peptides and prediction of bioactive potential

The protein (method n.960.52) and moisture (method n.925.45b) content of the samples was determined according to method described by Latimer (Association of Official Analytical Chemists, 2012). The factor of 6.38 was used to calculate the conversion of nitrogen to protein. Amino acids were determined using RP-HPLC column with 254 nm UV detector (Shimadzu Corporation, Tokyo, Japan), equipped with a C18 Luna/Phenomenex column (250 mm × 4.6 mm × , 5 μ; Phenomenex Inc., Torrence, USA). The identification and quantification was performed using a set of external standards (Pierce/PN, 20088), according to (Hagen et al., 1989) and (White et al., 1986).

The biological activity of peptides was predicted by BIOPEP® database (http://www.uwm.edu.pl/biochemia/index.php/pl/biopep, accessed on February 20, 2022). The molecular weight, isoelectric point (IP), net charge, and hydrophobicity of peptides were analyzed by PepDraw (http://www.tulane.edu/~biochem/WW/PepDraw/index.html, accessed on February 20, 2022). The amino acids were presented as one letter nomenclature.

2.3.1. Hydrolysate profile by high efficiency capillary electrophoresis (HPCE)

The whey protein hydrolysates (WPH) were analyzed in capillary electrophoresis system (Agilent Technologies, Waldbronn, Germany) equipped with UV detector and diode array, G2201AA Agilent ChemStation software for system control, analysis and collection of data. CE Conditions: The fused silica capillary length was 40 cm (Agilent Technologies, DE, Germany), 50 μm DI (internal diameter) and as a basic electrolyte a 20 M borate buffer solution pH 9 was used. The sample was injected at 20 kV for 20 s. The applied voltage was set at 15 kV, and a pressure of 50 mbar was applied to the inlet capillary during the run.

2.4. Synthesis of peptides-iron complexes and its binding capacity (solubility)

Peptides-iron complexes were synthesized using the hydrolysate fraction of peptides (<5 kDa adjusted to pH 5.5) and Fe from 0.1% (w/v) $FeSO_4$ aqueous solutions in a water bath with shaking for 30 min at 40 °C followed by centrifugation (5000 g/20 min, 25 °C). Several proportions of peptide: iron (w/w) 5:1; 10:1; 20:1 and 40:1 were evaluated to select the best ratio of peptides: iron (w/w) to be used for the synthesis of complexes (peptide-iron). The solubility of iron:peptide complexes was used to assess the binding capacity of iron on pH 5.0 and 7.0 (Hoz et al., 2014; Kim et al., 2007). After the synthesis of peptide-iron complexes at pH 5.0, part of the samples was adjusted to pH 7.0. The solubility of both samples (pH 5.0 and pH 7.0) was tested at several proportions of peptide: iron (w/w) 5:1; 10:1; 20:1 and 40:1. The best ratio of peptides: iron (w/w) was selected to be used in further analysis.

2.5. Iron solubility

Iron solubility technique was used to access the end process of peptide binding capacity, bioaccessibility, and bioavailability. The iron content in the sample and in the products of the chelation reaction was determined according to the method described by (Price and Roos, 1969) and modified by (Morgano et al., 1999), based on its solubility. The iron content was quantified using an inductively coupled plasma optical emission spectrometer (model 5100 DV ICP OES, Agilent Technologies, Tokyo, Japan), equipped with a 27 MHz solid state radiofrequency (RF) source using argon as plasma (purity 99.996% - Air Liquid, SP, Brazil) and seaspray nebulizer. The optimized operating conditions were: RF Power 1.20 kW; Auxiliary argon flow 1.0 L min^{-1}, nebulization flow 0.7 L min^{-1}, replicate number 3; Stabilization and reading time 14 s and wavelength 259.940 nm. The analytical curve was prepared by successive dilutions from an iron standard solution (1000 mg/100 mL, Titrisol-Merck, Darmstadt, Germany), ranging from 0.001 to 1.000 mg/100 mL ($r > 0.9999$). Quality control was performed in all batches using Fe-standard solutions.

2.6. Iron bioaccessibility

Iron bioaccessibility was measured in Fe-peptide complexes, microparticles and formulations. The bioaccessibility was evaluated according

to (Argyri et al., 2009), which allows the analysis to be carried out with a reduced amount of sample. The *in vitro* dialyzability method simulates gastrointestinal digestion and a specific porosity membrane (6–8 kDa) simulates the intestinal wall. The calculation of % iron dialyzability in the samples is obtained using the formula:

$$\%\ \text{Iron dializability} = \frac{\textbf{Iron dialisate } \left(\frac{\textbf{mg}}{\textbf{mL}}\right) \text{ x } \textbf{vol total}}{\textbf{\textit{Initial Iron total}} \ (\textbf{\textit{mg}})} \times 100$$

where:

$$\text{Iron dializability (mg/mL)} = \frac{\textit{Iron mg of dialisate}}{\textit{dialisate volume}} = \frac{\textit{Iron}\left(\frac{mg}{100mL}\right) \textit{x factor}}{\textit{dialisate volume}}$$

- Dialysate volume: weighing of the dialysate mass (content above the membrane in the insert) expressed in mL; Initial total Iron: 0.0224 mg (Argyri et al., 2009).

2.7. Iron bioavailability

Iron bioavailability was measured in Fe-peptide complexes, microparticles, and formulations. The samples passed through a digestion process and after through Caco-2 cells cultured assay. The *in vitro* digestion was performed according to the Infogest protocol with modification (Minekus et al., 2014), which is composed of three stages: (1) preparation of stock solutions; (2) preparation of solutions for digestion; (3) simulation of gastrointestinal digestion.

For the bioavailability assays, polyester membrane filters of inserts or Transwell® inserts (0.4 μm pores, 4.7 cm^2 growth area; Corning Life Sciences, Acton, MA, USA) inside 6-well Snapwell cell culture chambers were used in transport and uptake experiment. Transwell dish was constituted with an apical compartment (AP) and a basolateral compartment (BL), separated by a porous membrane containing approximately 1.0×10^5 cells/cm^2. The Caco-2 cells were cultured for 15 days until a total confluence monolayer was formed. The culture media (1.5 mL in the insert and 2.5 mL in the well) were changed every 2 days and the transepithelial electric resistance (TEER) between AP and BL was regularly monitored with a Millicell® electrode resistance system (Millipore Iberia, Madrid, Spain) to test the integrity of the monolayer.

The measurements of iron bioavailability were done considering its concentration at the BL compartment. Before the experiment, the TEER was verified as being greater than 250 Ω cm^2 (Do Nascimento da Silva and Cadore, 2019). The cell monolayer was rinsed two times with DPBS solution (Dulbecco's Phosphate Buffered Saline) incubated with 1.5 mL chyme (0.12 mg/mL of total iron concentration) in AP and with Hanks buffered salt solution (HBSS) in BL for 4 h at 37 °C. The osmolality of the chyme was measured (semi-micro osmometer, model K 7400, Knauer, Berlin, Germany) and presented a mean value close to 310 mOsm/kg, which is the recommended value of solutions used with Caco- 2 cells (Do Nascimento da Silva and Cadore, 2019). At the end of the experiment, the resulting liquids of the AP and BL compartments were aspirated and reserved for analysis by ICP OES.

2.8. Production of microparticles

After defining the best proportion for the synthesis of iron-peptide complexes, which have been termed "active" (iron-peptide and ascorbic acid), their complexation was performed according to the method described by (Filiponi et al., 2019).

2.9. Morphology and microstructure

The microparticles microstructure *(Fe-peptides and peptides) were evaluated by scanning electron microscopy (SEM, DSM 940A, ZEISS, Jena, Germany) and X-ray microanalysis by energy dispersion (EDX). Before imaging, the sample was spread on a glass slide fixed on the specimen holder and sputter-coated with gold. After SEM evaluation, the same samples were subjected to the EDX analysis to verify the elements present at the particles surface, in an equipment model Link Isis Oxford Instruments.*

2.10. Microparticles formulation

The microparticles were used for the preparation of three formulations: *strawberry, tangerine and chocolate. The concentration of iron in the microparticles (Fe^{2+}) was* 14 mg *per sachet, based on the daily recommended ingestion* (DRI, 2006) *for adults. Thus, the ingredients selected were those that did not interfere with absorption of the iron or even presented a synergic effect to improve iron absorption. These microparticles were evaluated in previous studies, showed an increase in iron bioavailability (De la* Hoz et al., 2014*;* Caetano-Silva et al., 2017; Cruz-Huerta et al., 2016). Flavors, sugar, citric acid and flavoring were used to compose a sachet are showing with details in Audiverth et al. (2021).

2.11. Molecular docking

The interaction between ferric iron (Fe^{2+}) and peptides from whey isolate and fractionation were evaluated by molecular coupling. The peptides and Fe^{2+} were designed using Instant MarvinSketch (ChemAxon Ltd). Flexible torsions, charges, and the grid size were assigned by AutoDock Tools (Morris et al., 2009) and the docking calculations were performed using AutoDock Vina (Oleg and Arthur, 2010). The peptide-Fe^{2+} interaction with the lowest estimated free energies (EFE), which means the highest binding affinity, was selected as a representative image to visualize in the Discovery Studio 2016 Client (Dassault Systemes Biovia Corp.).

2.12. Statistics evaluation

The results were evaluated by one-way ANOVA and Tukey test with 95% of confidence and the dates were organized by XLSTAT software, Addinsoft, Paris, France.

3. Results

3.1. Characterization of hydrolysate and fraction profile

The fraction < 5 kDa of WPI hydrolysates presented 2.4 ± 0.4% of moisture and 96.5 ± 0.7% of protein. The amino acids profile (Table 1) shows that predominant free amino acids were in the following order of concentration: phenylalanine, isoleucine, leucine, lysine, and cystine. The determination of free amino acids was important to demonstrate that they are in a minute fraction of the hydrolyzate < 5 kDa (Table 1) reaching a mass of approximately 1.0% of the total (944.63 mg/100g of hydrolyzate) and thus do not compete with the peptides for the iron.

Previous studies performed by our group carried out amino acid sequencing of smaller peptides (WPH <5 kDa) with iron ion affinity (IMAC-Fe III) by mass spectrometry (Cruz-Huerta et al. 2016). The results demonstrated that the peptides had common characteristics, such as, high levels of aspartic acid, glutamic acid and many of them with the amino acid proline. A meaningful part of the iron-binding peptides could be identified as coming from b-lactoglobulin (b-Lg), the predominant protein of whey protein. Most of the peptides identified were originated from a specific region (42–59/q122-137). Therefore, it was hypothesized that the key role of Asp, Glu and Pro in the chelation of iron has been reported previously, when the Asp and Glu form very stable Fe-chelates probably with a tridentate structure. Due to the cyclic nature of the PRO amino acid it can contribute by enhancing resistance to digestion enzymes (Nelson and Cox, 2016; Cruz-Huerta et al., 2016).

Our previous studies have identified some peptides with Pro and the respective molecular weights: VEELKPTPEGDLE (1454.71 MW);

Table 1
Total and free amino acids from total whey hidrolysed and its fraction <5 kDa.

Amino Acid (AA)	WH* Alcalase	WHP** Alcalase (<5 kDa)	
	Total AA (g/100 g sample)		Free AA (mg/100g sample)
Acids + Amides			
Aspártico Acid	11,80 ± 00,3	12,34 ± 0,02	36,40 ± 0,12
Glutamic Acid	17,46 ± 0,06	18,62 ± 0,01	8,89 ± 0,02
Aliphatics amino acids			
Alanine	4,20 ± 0,02	5,46 ± 0,01	17,31 ± 0,05
Glicine	1,61 ± 0,00	1,87 ± 0,01	2,88 ± 0,00
Isoleucine	4,72 ± 0,01	6,48 ± 0,01	205,55 ± 0,64
Leucine	11,63 ± 0,01	11,67 ± 0,01	154,57 ± 0,36
Valine	4,68 ± 0,02	4,95 ± 0,01	7,80 ± 0,39
Aromatics amino acids			
Phenylalanine	3,01 ± 0,00	2,91 ± 0,00	222,28 ± 2,34
Tirosina	3,31 ± 0,00	2,43 ± 0,05	4,80 ± 1,11
Tryptophan	1,19 ± 0,03	Nd	99,30 ± 0,38
Hydroxylated amino acids			
Serine	4,02 ± 0,01	3,88 ± 0,00	7,59 ± 0,01
Threonine	5,17 ± 0,00	4,59 ± 0,00	68,34 ± 0,13
Sulfur amino acids			
Cysteine	0,68 ± 0,05	1,28 ± 0,16	19,81 ± 0,02
Methionine	2,85 ± 0,01	2,78 ± 0,07	19,74 ± 0,10
Imino acids			
Poline	3,79 ± 0,01	3,60 ± 0,01	2,53 ± 0,06
Basics amino acids			
Arginine	2,58 ± 0,02	2,02 ± 0,00	14,52 ± 0,00
Histidine	1,87 ± 0,00	2,12 ± 0,01	25,87 ± 0,03
Lysine	9,79 ± 0,02	9,47 ± 0,02	125,79 ± 0,85
∑ AA	93,17	96,43	944,63

* WH = WPI hydrolysates by Alcalase;** WHP= Whey hydrolyzed fraction (<5 kDa)

ELKPTPEGDLE (1226.60 MW); LKPTPEGDLE (1097.56 MW); LVRTPEVDDE (1171.57); DTDYKKY (931.43); RTPEVD (715.35) and KTKIPAVF (902.56). Other studies have also found two different peptides: VEELKPTPEGDLEIL (1681,88) LSFNPT (678,34) (Caetano-Silva et al. 2020).

Among the identified peptides sequences from WPI hydrolysates isolated by IMAC, the peptides LLR and VEELKPTPEGDLEIL had the lowest and highest molecular weight, respectively. Furthermore, the LLR peptide showed the highest IP in comparison with other sequences, while DISLL had the lowest. The net charge ranged between 2 and - 4 and the hydrophobicity was the highest in VEELKPTPEGDLE and the lowest in LIVTQ. As the main biological activities, all the peptides had ACE inhibitor, glucose update stimulation, and dipeptidyl peptidase (DPP IV) inhibitor activities and 38% of sequences presented antioxidant activity (Table 2).

The electropherogram (Fig. 1A and B) shows the hydrolysate profile using the alkalase® enzyme and amino acid distribution, respectively. This analysis evaluated differences on structure, size and load of hydrolyzed peptides. The highest concentration of peptides in our hydrolysates occurred in the intermediate region (5–7 min) indicating intermediate hydrophobicity.

3.2. Peptide-iron binding capacity

The peptide iron binding capacity was tested by iron solubility. It was assumed that iron is only soluble in the solution if attached to peptides (Fig. 1C). This analysis showed differences in iron solubility regarding pH and peptide: iron ratio. As observed in Fig. 2 at pH 5.0, iron was soluble above 60% both in the free iron from ferrous sulfate (control, 73.1% ± 3.1) and when bound to the peptide. However, the solubility of iron increased above 85% after peptide complexation in the proportions 10:1, 30:1 and 40:1.

At pH 7.0, the solubility of iron at ferrous sulfate form is drastically reduced but increases considerably (above 90%) after peptide complexation in the proportions 20:1, 30:1 and 40:1. These analysis show that peptide complexation has a pivotal role on iron solubility. Still, the intestinal pH (7,0) showed higher solubility then pH 5.0. Therefore, intestinal conditions seem to favors the stability of iron complexation.

3.3. Dialysability and estimation of the bioavailability of iron-peptide complexes in different peptide: iron proportions

The iron-peptide complexes were tested for dializability using a specific porosity membrane after *in vitro* digestion according to (Argyri et al., 2009) and by bioavalability, using the Caco-2 cells model (Do Nascimento da Silva and Cadore, 2019) after gastrointestinal digestion, using Infogest protocol (Minekus et al., 2014). Note that both protocols submit the sample to mimic physiological pH condition along the gastrointestinal (GI) tract (mouth - pH 7.0; gastric – pH 3.0 and intestinal - pH 7.0) and the end process should reflect the stability of the complex after adverse gastrointestinal conditions. The description process is shown in Fig. 2 and the results of iron peptide complexes are shown in Table 3. The values obtained indicate that samples with different proportions of peptides: iron (10:1 and 40:1) presented good percentages of the dialyzed iron (49.0 ± 5.0 and 46.7 ± 3.4), significantly different from the ferrous sulfate control sample, which presented very low dialysability (12.9 ± 0.0).

The assessment of bioavailability using Caco-2 cells showed similar results, which a higher percentage of bioavailability in iron-peptide complexes at different proportions 10:1 (56.2 ± 6.8) and 40:1 (2.9 ± 9.9), in opposite to iron sulfate control, which showed lower bioavailability of iron (9.6 ± 0.1).

Once we had a good dializability and bioavailability with 10:1 rate, which corresponds to the minimum proportion to obtain the best results, we continued with this concentration in the next experiments with microparticle.

3.4. Microparticles: morphology and microstructure

Scanning electron microscopy (SEM) analysis was used to assess the appearance of the microparticles. They showed a spherical shape, characteristic of powders produced by atomization. The energy scattering X-ray microanalysis (EDX) coupled to the SEM equipment was used to obtain information on the elemental composition of the surface material of the microparticles. Fig. 1111A shows the morphology of the microcapsules and Fig. 1C the EDX spectrum for the sample containing the iron-peptide complexes and the one containing only the peptide. The elements sodium (Z = 11) and chlorine (Z = 17) were detected possibly as a result of pH adjustment with HCl and NaOH solutions during the complex synthesis reaction (pH 5.0). Peptide nitrogen was not detected due to its low atomic number (Z = 7). It was also possible to identify the iron ion (Z = 26) on the surface of the microparticle structure with Fe-peptide, which can be either free or bound. Bearing in mind that iron has 4 or 6 sites to be coordinated with peptides, we can consider in this case that these may be fully or partially occupied. Therefore, these iron ions present on the surface are probably less likely to react with other compounds, according to Caetano-Silva et al. (2018) in a model system similar to this study.

3.5. Bioaccessibility and bioavailability studies of microparticles

The iron needs to be in ferrous form to ensure its solubility and absorption. Therefore, ascorbic acid (AA) in a proportion 1:1.6 (AA:Fe) was added before the drying process, as iron absorption increase by the reduction mechanism involving the conversion of ferric to ferrous form and avoiding oxidative damage by free soluble iron (Shubham et al., 2020). This mixture was called “active”. The yield of the process, considered as the percentage of active present in the feed solution and that recovered in the dry form, was 82%. %. The description process is shown in Fig. 3.

The iron bioaccessibility and bioavailability estimation were carried out with iron peptide microparticles to verify if the wall material used

Table 2
Main characteristics and biologic activity of peptides from total whey hidrolysed fraction <5 kDa.

Peptide	Molecular mass (Da)	IP	Net Charge	Hydrophobicity	Activity	Sequence
LIVTQ	572.35	5.48	0	6.09	ACE inhibitor	TQ, LIVTQ
					Glucose uptake stimulating peptide	IV, LI
					DPP IV inhibitor	LI, TQ, VT
LLR	400.28	10.73	1	7.21	ACE inhibitor	LR
					Glucose uptake stimulating peptide	LL
					Antioxidant	LLR
					DPP IV inhibitor	LL, LR
					Renin inhibitor	LR
LSFNPT	677.33	5.47	0	6.64	ACE inhibitor	SF, PT
					DPP IV inhibitor	NP, FN, PT, SF
					Renin inhibitor	SF
KVLVL	570.41	10.14	1	7.28	ACE inhibitor	LVL
					Glucose uptake stimulating peptide	VL, LV
					DPP IV inhibitor	KV, LV, VL
SDISLL	646.35	3.05	−1	8.84	Glucose uptake stimulating peptide	LL
					Regulator of phosphoglycerate kinase activity	SL
					DPP IV inhibitor	LL, SL
VEELKPTPEGDLEIL	1680.87	3.48	−4	25.21	ACE inhibitor	LKP, GD, EG, KP, EI, VE, PT, TP, IL
					Glucose uptake stimulating peptide	IL
					Stimulating vasoactive substance release	EE
					Stimulating GLP-1 release	LKPT
					Antioxidant	LKP, LK, KP
					DPP IV inhibitor	LKPTPEGDL, LKPTPEGDLEIL, TP, KP, EG, EI, IL, PT, VE
					Alpha-glucosidase inhibitor	VE, PE
					DPP-III inhibitor	PE
DISLL	559.32	2.95	−1	8.38	Glucose uptake stimulating peptide	LL
					Regulator of phosphoglycerate kinase activity	SL
					DPP IV inhibitor	LL, SL
DEIQVLLVL	1040.60	2.82	−2	10.15	ACE inhibitor	LVL, EI
					Glucose uptake stimulating peptide	LV, LL
					DPP IV inhibitor	EI, IQ, LV, QV, VL
VEELKPTPEGDLE	1454.71	3.48	−4	27.58	ACE inhibitor	LKP, GD, EG, KP, VE, PT, TP
					Stimulating vasoactive substance release	EE
					Stimulating GLP-1 release	LKPT
					antioxidative peptide	EL, LKP, LK, KP
					DPP IV inhibitor	LKPTPEGDL, TP, KP, EG, PT, VE
					Alpha-glucosidase inhibitor	VE, PE
					DPP-III inhibitor	PE
ELKPTPEGDLE	1226.60	3.57	−3	24.71	ACE inhibitor	LKP, GD, EG, KP, PT, TP
					Stimulating GLP-1 release	LKPT
					Antioxidative peptide	EL, LKP, LK, KP
					DPP IV inhibitor	LKPTPEGDL, TP, KP, EG, PT
					Alpha-glucosidase inhibitor	PE
					DPP-III inhibitor	PE
LKPTPEGDLE	1097.55	3.74	−2	20.78	ACE inhibitor	LKP, GD, EG, KP, PT, TP
					Stimulating GLP-1 release	LKPT
					Antioxidative peptide	LKP, LK, KP
					DPP IV inhibitor	LKPTPEGDL, TP, KP, EG, PT
					Alpha-glucosidase inhibitor	PE
					DPP-III inhibitor	PE
LVRTPEVDDE	1171.57	3.54	−3	22.47	ACE inhibitor	LVR, VR, LVRT, EV, TP
					Glucose uptake stimulating peptide	LV
					DPP IV inhibitor	VR, EV, LV, VD
					Alpha-glucosidase inhibitor	PE
					DPP-III inhibitor	PE
DTDYKKY	931.42	6.61	0	19.61	ACE inhibitor	KY, YK, DY
					Peptide regulating ion flow	DY
					Antioxidant peptide	TDY, DYK, KKY, KK
					DPP IV inhibitor	KK, KY, TD, YK
					DPP-III inhibitor	YK
RTPEVD	715.34	4.00	−1	16.91	ACE inhibitor	EV, TP
					DPP IV inhibitor	TP, EV, VD
					Alpha-glucosidase inhibitor	PE
					DPP-III inhibitor	PE
KTKIPAVF	902.55	10.59	2	11.10	ACE inhibitor	VF, IPA, IP, AV
					DPP IV inhibitor	PA, IPA, IP, IPAVF, AV, KI, KT, TK, VF
VEELKPTPEGDLEIL	1680.87	3.48	−4	25.21	ACE inhibitor	LKP, GD, EG, KP, EI, VE, PT, TP, IL
					Glucose uptake stimulating peptide	IL

(*continued on next page*)

Table 2 (*continued*)

Peptide	Molecular mass (Da)	IP	Net Charge	Hydrophobicity	Activity	Sequence
					Stimulating vasoactive substance release	EE
					Stimulating GLP-1 release	LKPT, KPT
					antioxidative peptide	LKP, LK, KP
					DPP IV inhibitor	LKPTPEGDL, LKPTPEGDLEIL, TP, KP, EG, EI, IL, PT, VE
					Alpha-glucosidase inhibitor	VE, PE
					DPP-III inhibitor	PE
LSFNPT	677.33	5.47	0	6.64	ACE inhibitor	SF, PT
					DPP-III inhibitor	PT, NP, FN, SF
					Renin inhibitor	SF

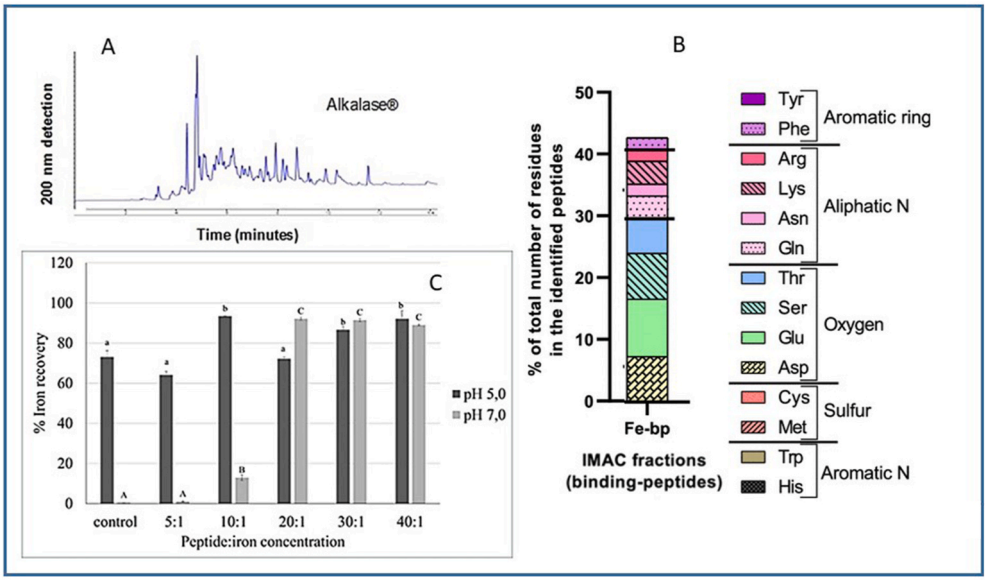

Fig. 1. A) Electrophoretic profile of hydrolysates by HPCE. B) Amino Acids distribution and, C) Solubility of Fe-peptides under different pH conditions (5.0 and 7.0).

would not interfere with the release of iron. As shown in Table 4, the solubility of iron after microparticle gastrointestinal digestion was higher than the control (39.1 ± 2.3 and 10.1 ± 0.7, respectively), as it was in dializability analysis (19.8 ± 1.2 and 12.8 ± 1.8, respectively) and bioavailability (34.8 ± 0.2 and 9.7 ± 0.0).

3.6. Formulations study: bioaccessibility and bioavailability tests

The microparticles were used to make powder formulations for beverages. After spray dryer process the determination of the iron content by ICP OES served to estimate the necessary amount of microparticles to compose the formulations described by (Audiverth et al., 2021).

The results of the microparticles formulations are shown in Table 5. The sample of iron sulfate used as a control presented less solubility than the formulations. Our results showed that the bioacessibility by two methods (solubility after digestion and dializability) and bioavailability were higher in tangerine (85.7%; 36.7%; 80.5%) and strawberry formulation (90.9%, 29.9%, 84.1%) than in chocolate formulation (36.5%, 14.3%, 33.6%). The lower levels of dializability was probably because of the incomplete digestion procedure of ARGYRI digestion.

3.7. Molecular docking

It was observed that every described peptides interacted with Fe^{2+}, once all sequences showed negative values of EFE. However, the peptide ELKPTPEGDLE demonstrated the highest interaction, because it demonstrated the lowest binding energy (EFE −1.2) (Fig. 4).

4. Discussion

To our best knowledgement, there are no studies in the literature, which evaluate the bioaccessibility and bioavailability of iron-complexes after microencapsulation and incorporation into formulation. Our hydrolysates of whey protein with alcalase generated peptides with high levels of phenylalanine, isoleucine, leucine, lysine, and cystine. This result reflects the enzyme's action in preferentially cleaving hydrophobic groups. In general, they are amino acids with functional groups capable of forming coordinated covalent bonds (Hoz et al., 2014; Ou et al., 2010; Wu et al., 2012). The iron-binding capacity of peptides is determined by the spatial distribution of functional groups of the amino acids in the peptide sequence, and their interactions are influenced by the amino acid sequence (Carlton and Schug, 2011). This binding between the WPI hydrolysates peptides with iron, forming a chelate, was confirmed by *in silico* analysis, given that all peptides showed interaction with Fe^{2+}. Amino acids and protein digestion products, such as small peptides, are excellent ligands because they have at least two functional groups (amino and hydroxyl), allowing the formation of a ring structure. At neutral intestinal conditions the Fe solubility is extremely reduced, and is the main factor for the lower bioavailability. Chelating ligands protect the iron from binding with water, thereby hindering the formation of ferric hydroxides and increasing iron solubility (Zhu et al., 2009). Furthermore, the synthesis of the peptide-iron complex before the digestion process may protect

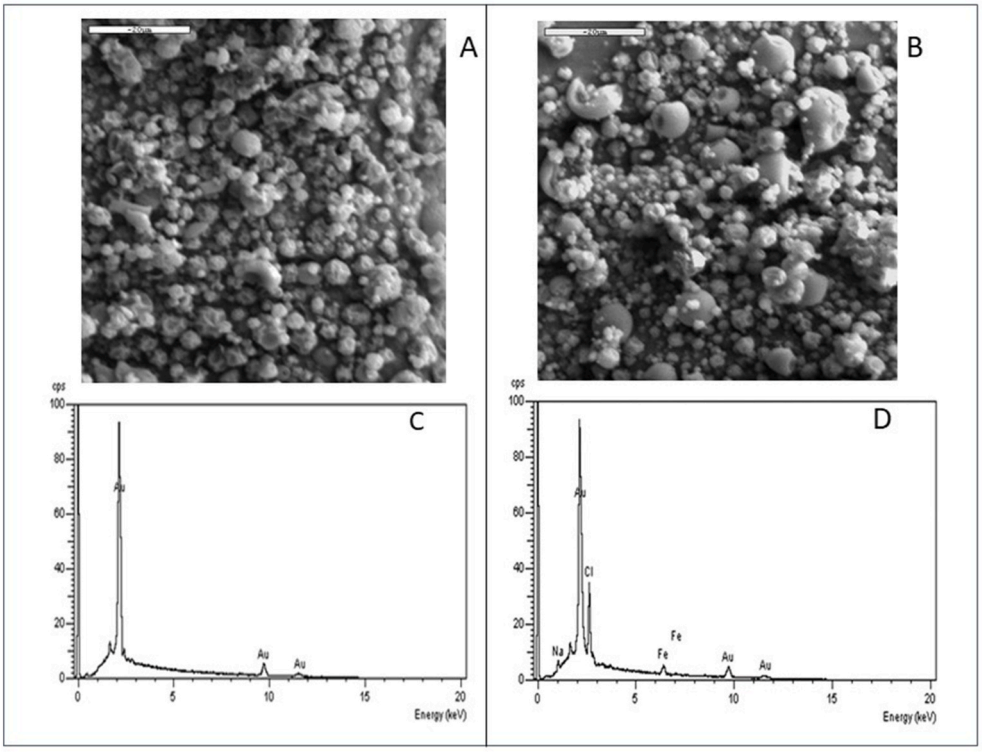

Fig. 2. Morphology and microstructure of the microparticles. A) with Fe-peptides; B) only peptides without Fe; C) elemental composition of the surface material of the microparticles for the sample containing the iron-peptide complexes and D) the one containing only the peptide.

Table 3
Iron dializability of samples with different peptide ratios and estimation of iron bioavailability in a transwell model with CACO-2 cell line, for different peptide: iron ratios.

Ratios	% Fe*	
Iron: peptide complexes	Dializability[1]	Bioavalability[2]
10: 1	49.02 ± 5.0 ^{B}	56.23 ± 6.7 ^{B}
40: 1	46.76 ± 3.4 ^{B}	24.97 ± 9.9 ^{B}
Control ($FeSO_4$)	12.81 ± 1.8 ^{A}	9.74 ± 0.1 ^{A}

* Average value of three measurements (n = 3) and standard deviation (SD) with confidence level of 95%; [1]Argyri et al., 2009; [2]do Nascimento da Silva & Cadore, 2019.

against adverse gastrointestinal conditions. Acidic stomach conditions are not favorable for the formation of the complex with the peptide, since the binding sites of the metal must be protonated, inhibiting the interaction between the peptide and the metal ion (Caetano-Silva et al., 2020).

In the present study the Fe-peptide complexation increased solubility either on pH 5.0 and 7.0. It is already known that reduction in iron solubility occurs due to the different pH conditions faced during digestion in the gastrointestinal tract (Salovaara et al., 2002). Therefore, ferrous iron precipitates at neutral pH values (7.0) and may remain soluble only if chelated (Salovaara et al., 2002). On the other hand, ferric iron precipitates as hydroxides at pH values above 4 and, therefore, needs to be chelated in the stomach or in the proximal duodenum to remain in a dissolved state (Conrad and Umbreit, 2000). Our results showed that iron peptide complexation was really effective on maintaining iron solubility, especially on physiological pH 7.0. These results were confirmed by the isoelectric point of most of the peptides obtained being out of the range of pH between 5.0 and 7.0, thus avoiding the precipitation of peptides and collaborating in the solubility of the peptide:iron chelate. Furthermore, the results of this study showed that Fe-peptide complexation increased iron bioaccessibility and bioavailability compared to free-iron form. Similar results were found by Hoz et al. (2014) who described the dialyzability of whey peptide samples obtained from <5 kDa fractions complexed with iron were superior to the control sample of ferrous sulfate. The analysis of dialyzability usually indicates that amounts of soluble and stable iron remain as such until the time of intestinal digestion (Hoz et al., 2014). Although the dialysis capacity of iron does not define the level of iron absorption, it is an acceptable indicative of an absorbable condition and is a suitable method for the rapid screening of a large number of samples before proceeding to human trials (Aragón et al., 2012; Argyri et al., 2011). Furthermore, the Argyri et al. (2009) method is recommended because uses less samples, reagents and supplies than other *in vitro* methods previously described, as Minekus et al., 2014. In addition, it requires a sensitive method for iron determination.

Related to bioavailability results we also obtained a good iron solubility in this analysis, suggesting that after the digestion process, the iron-peptide complexes may cross the enterocyte barrier and exerting beneficial effects. After pass and resist through the gastrointestinal digestion, the metal is likely to remain bound to the peptide and be absorbed through the same peptide route, although this requires further investigation (Caetano-Silva et al., 2020). In agreement with these hypotheses, previously work showed that smaller peptide complexed with iron (<5 Kda) presented better Fe uptake by Caco-2 cells than larger peptides (>5 Kda) with similar sequences, suggesting that iron absorption is highly dependent on peptide absorption (Caetano-Silva et al., 2018).

Moreover, the low hydrophobicity of most of the identified peptides can directly contribute to the greater absorption of the chelate in intestinal cells. It is demonstrated that peptides with hydrophobicity ≤20 kcal/mol are more effective in penetrating the cell membranes and consequently performing activities (Mojica et al., 2017). Some of these biological effects were presumed, based on bioinformatics analysis. It was found that all peptides had ACE and DPP-IV inhibitory and glucose regulating effects, which presupposes benefits regarding arterial hypertension and diabetes mellitus (Muñoz et al., 2018). In addition, many

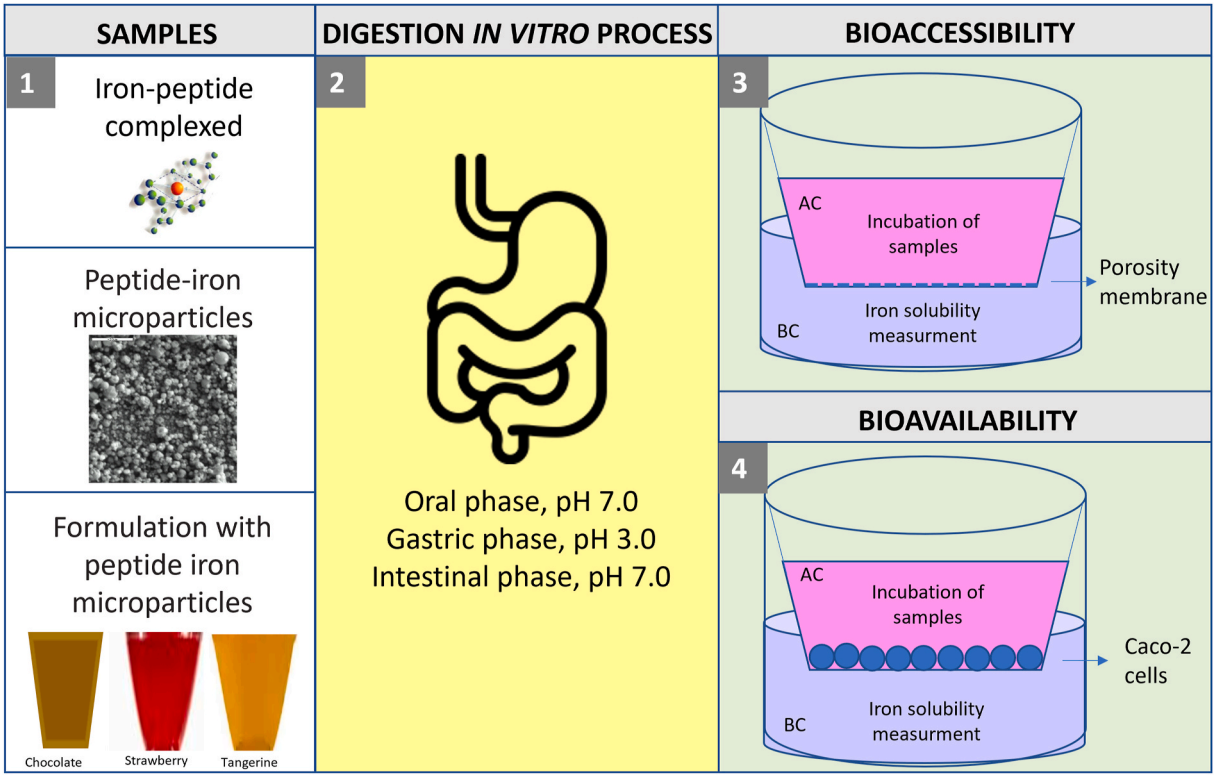

Fig. 3. Experimental representation of the process steps.

Table 4
Bioaccessibility tests and bioavailability estimate with samples of microparticles.

Sample	(%) **Fe** ± DP*		
	BIOACCESSIBILITY		BIOAVAILABILITY
	Solubility[1]	Dialyzability [2]	Caco-2 Cell[3]
Microparticle	39.10 ± 2.3 ^{B}	19.84 ± 1.2 ^{A,B}	34.87 ± 0.2 ^{B}
Control ($FeSO_4$)	10.17 ± 0.7 ^{A}	12.86 ± 1.8 ^{A}	9.70 ± 0.1 ^{A}

* Average value of three measurements (n = 3) and standard deviation (SD) with confidence level of 95%. Diferent superscript letters on the same row are significant by different at $p < 0.05$; [1] Iron solubility after digestion by Minekus et al. (2014); [2] Dializability by Argyri et al. (2009); [3]Caco-2 cell after digestion by Minekus et al. (2014).

Table 5
Bioaccessibility and bioavalability of iron in powder formulations for beverages after digestion.

Samples	% Fe ± SD *		
Formulation	BIOACCESSIBILITY		BIOAVALABILITY
	Solubility [1]	Dializability [2]	Caco-2 cell [3]
Tangerine	85.76 ± 0.5 ^{c}	36.76 ± 4.0 ^{C}	17.96 ± 3.8 ^{B}
Strawberry	90.91 ± 1.2 ^{c}	29.98 ± 3.2 ^{B,C}	20.90 ± 1.6 ^{B}
Chocolate	36.58 ± 2.1 ^{B}	14.31 ± 1.1 ^{A}	4.32 ± 0.5 ^{A}
Control (Fe SO_4)	10.17 ± 0.7 ^{A}	12.86 ± 1.8 ^{A}	0.75 ± 0.2 ^{A}

* Average value of three measurements (n = 3) and standard deviation (SD) with confidence level of 95%. Diferent superscript letters on the same row are significant by different at $p < 0.05$; [1] Iron solubility after digestion by Minekus et al. (2014); [2] Dializability by Argyri et al. (2009); [3]Caco-2 cell after digestion by Minekus et al. (2014).

peptides have demonstrated antioxidant effects, being able to combat the formation of reactive oxygen species (ROS) that are directly related to the development of diseases and metabolic body complications Grancieri et al. (2019). Therefore, it is now possible to contribute with the literature, attributing a new characteristic regarding the binding capacity of this peptides with iron.

Caco-2 cells are recognized as a good cellular model of intestinal enterocytes that simulates the intestinal barrier (Fabiano et al., 2018). Although the number of studies using Caco-2 cells has increased in recent years, there are still limitations in their use. For iron, for example (as in the case of this work), other organs are involved in the regulation of the nutrient absorption process, such as the liver, which is not taken into account in the studies carried out with these cells (Scheers et al., 2014).

Thus, bioavailability tests should be used as an estimative of how much the element would be absorbed by the intestine during digestion and not to predict the real value. Some studies carried out a comparative study of the bioavailability of iron between *in vitro* and *in vivo* methods with humans, finding a good correlation (r = 0.9765; P = 0.0008) (Aragón et al., 2012). They concluded that in some cases, even if the correlation is not so close, it may indicate a similar trend to the *in vivo* results in relation to ferrous sulfate. The method by which iron is transported through the intestinal cell membrane has not been sufficiently studied, and more research must be carried out to clarify this mechanism (Li et al., 2017).

Our results regarding the formation of microparticles with iron-peptide complexes did not negatively interfere with the solubility of iron, a predictive condition for its absorption (Hoz et al., 2014), thus being able to be used for the synthesis of formulations. In the analysis with formulations and microparticles, the bioacessibility and bioavailability of strawberry and tangerine presented higher iron solubility than chocolate formulation. These results could be explained because of the presence of ascorbic acid and sugars in strawberry and tangerine formulas, which may act as protectors against iron oxidation. Ascorbic acid is known to be the most efficient promoter of iron absorption, mainly for

Peptide	EFE
LIVTQ	-1.0
LLR	-0.6
LSFNPT	-0.9
KVLVL	-1.1
SDISLL	-0.9
VEELKPTPEGDLEIL	-1.0
DISLL	-0.9
DEIQVLLVL	-1.1
VEELKPTPEGDLE	-1.0
ELKPTPEGDLE	**-1.2**
LKPTPEGDLE	-1.0
LVRTPEVDDE	-1.1
DTDYKKY	-0.9
RTPEVD	-1.0
KTKIPAVF	-1.1
VEELKPTPEGDLEIL	-1.1
LSFNPT	-0.8

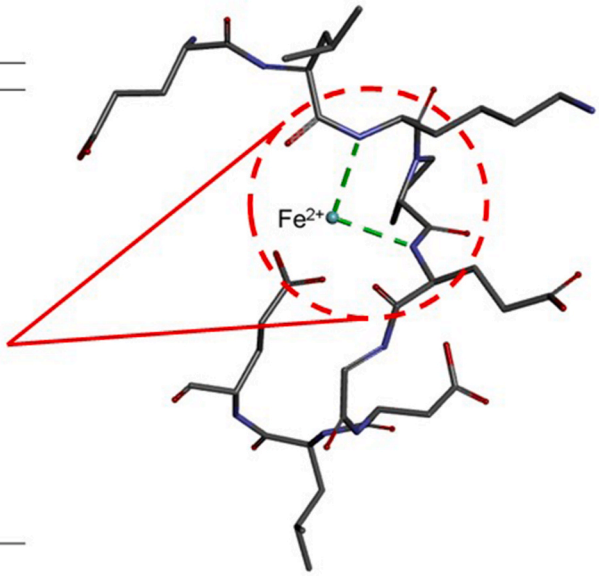

Fig. 4. The *in silico* interaction between peptides from whey isolate and fractionation and ferric iron (Fe^{2+}). Dates analyzed by AutoDock Vina®. Negative values mean spontaneous reaction. The most potent interaction between peptides and Fe^{2+} is in bold and is visualized using Discovery Studio 2016 Client®. The amino acids are presented in one letter nomenclature: A = Ala; C = Cys; D = Asp; E = Glu; F = Phe; G = Gly; H = His; I = Ile; K = Lys; L = Leu; M = Met; N = Asn; P = Pro; Q = Gln; R = Arg; S = Ser; T = Thr; V = Val; W = Trp; Y = Tyr. EFE: estimated free energy.

its reduction capacity through its hydroxyl groups (Salovaara et al., 2002; Trijatmiko et al., 2016). Furthermore, sugar is able to chelate inorganic iron and form stable and soluble complexes with low molecular weight (Charley et al., 1963; Christides and Sharp, 2013). These iron-sugar complexes showed to be readily absorbed through the intestinal mucosa of rodent models (Charley et al., 1963; Christides and Sharp, 2013). The most consistent finding in relation to mono- and disaccharides and iron is that fructose increases the dietary absorption of non-heme iron, possibly by chelation and/or reduction of iron to the ferrous form, increasing its solubility and permeability in the enterocyte (Christides and Sharp, 2013). Afterwards, the presence of cocoa and xanthan gum in the chocolate formulation may be related to its low iron bioaccessibility (Ma et al., 2010).

In this study, formulations containing microparticles with Fe-peptide complexes were produced, which may represent beverage with health benefits actions on iron deficiency combat. Our formulation presents two important aspects, such as high solubility that may decreases the formation of reactive oxygen species which cause side effects and damage to the intestinal cells (Guzun-Cojocaru et al., 2011; Sugiarto et al., 2010). Furthermore, the higher bioavailability may indicate how much of this mineral will reach the cells and play their physiological role.

5. Conclusions

The iron-whey peptides complexes were stable and able to increase the iron solubility even at physiological pH (7.0) and present higher rates of dializability and bioavailability after two *in vitro* digestion methods. Furthermore, the production of microparticles and their incorporation into formulations proved to be an effective way to increase the iron bioaccessibility and bioavailability and represents an alternative to protect the mineral besides to mask undesirable flavors. The 10:1 peptide: iron ratio showed a desirable performance in the complexation reaction with iron. The microparticles presented a better performance than the control sample, regarding the iron bioaccessibility tests. The ARGYRI method proved to be predictive for the cell model with Caco-2 cells. The presence of ascorbic acid, citric acid and sugars, in the formulations of tangerine and strawberry, contribute to increase the absorption of iron, according to the results obtained for the bioaccessibility and bioavailability of the mineral. The chocolate flavor did not show a favorable performance probably due to the addition of cocoa and gums to provide the characteristic viscous consistency of the drink. The microencapsulation process of the peptide: iron complex is important to enable its use as an active ingredient in other formulations and promotes greater bioaccessibility when incorporated into formulations.

CRediT authorship contribution statement

Bruna Gaigher: Investigation, Methodology, Formal analysis, Investigation, Writing – original draft. **Emanueli do Nascimento da Silva:** Investigation, Formal analysis. **Vitor Lacerda Sanches:** Investigation. **Raquel Fernanda Milani:** Investigation, Formal analysis, statistical analysis. **Fabiana Galland:** Investigation, Formal analysis, Writing – review & editing. **Solange Cadore:** Funding acquisition, Resources, Writing – review & editing. **Mariana Grancieri:** Formal analysis, Molecular docking, statistical analysis. **Maria Teresa Bertoldo Pacheco:** Conceptualization, Project administration, Funding acquisition, Resources, Writing – review & editing.

Declaration of competing interest

The authors declare the following financial interests/personal relationships which may be considered as potential competing interests:

Maria Teresa Bertoldo Pacheco reports equipment, drugs, or supplies, statistical analysis, and writing assistance were provided by Institute of Food Technology. All co-authors have seen and agreed with the contents of the manuscript and there is no financial interest to report. We certify that the manuscript contains original research and the submission is not under review at any other journal.

Acknowledgments

The authors gratefully acknowledge the São Paulo Research Foundation, FAPESP, São Paulo, Brazil (Process n° 2016/12660–3) for the financial support and scholarship (Proc. n° 2017/17554–0).

References

Abdel Moety, G.A.F., Ali, A.M., Fouad, R., Ramadan, W., Belal, D.S., Haggag, H.M., 2017. Amino acid chelated iron versus an iron salt in the treatment of iron deficiency anemia with pregnancy: a randomized controlled study. Eur. J. Obstet. Gynecol. Reprod. Biol. 210, 242–246. https://doi.org/10.1016/j.ejogrb.2017.01.003.

Antunes, S.A., Canziani, M.E.F., 2016. Hepcidin: an important iron metabolism regulator in chronic kidney disease. Jornal Brasileiro de Nefrologia 38 (3), 351–355. https://doi.org/10.5935/0101-2800.20160053.

AOAC, 2012. Official Methods of Analysis, nineteenth ed. Association of Official Analytical Chemists, Arlington, VA.
Aragón, I.J., Ortiz, D., Pachón, H., Arago, I.J., 2012. To Screen Iron Bioavailability, vol. 6337. https://doi.org/10.1080/19476337.2011.596283.
Argyri, K., Birba, A., Miller, D.D., Komaitis, M., Kapsokefalou, M., 2009. Predicting relative concentrations of bioavailable iron in foods using in vitro digestion: new developments. Food Chem. 113 (2), 602–607. https://doi.org/10.1016/j.foodchem.2008.07.089.
Argyri, K., Theophanidi, E., Kapna, A., Staikidou, C., Pounis, G., Komaitis, M., Kapsokefalou, M., 2011. Iron or zinc dialyzability obtained from a modified in vitro digestion procedure compare well with iron or zinc absorption from meals. Food Chem. 127 (2), 716–721. https://doi.org/10.1016/j.foodchem.2011.01.005.
Athira, S., Mann, B., Sharma, R., Pothuraju, R., Bajaj, R.K., 2021. Preparation and characterization of iron-chelating peptides from whey protein: an alternative approach for chemical iron fortification. Food Res. Int. 141, 110133. https://doi.org/10.1016/j.foodres.2021.110133. June 2020.
Audiverth, H.L.F., de Oliveira Garcia, A., de Salvucci Celeste Ormenese, R.C., Bertoldo Pacheco, M.T., 2021. Use of the Kano model and sensory evaluation in the development of an iron supplement for women. J. Sensory Stud. 36 (4), 1–14. https://doi.org/10.1111/joss.12655.
Blanco-Rojo, R., Vaquero, M.P., 2019. Iron bioavailability from food fortification to precision nutrition. A review. Innovat. Food Sci. Emerg. Technol. 51 (January 2018), 126–138. https://doi.org/10.1016/j.ifset.2018.04.015.
Caetano-silva, M.E., Bertoldo-Pacheco, M.T., Paes-leme, A.F., Maria, F., 2015. Iron-binding peptides from whey protein hydrolysates : evaluation , isolation and sequencing by LC – MS/MS. FRIN 71, 132–139. https://doi.org/10.1016/j.foodres.2015.01.008.
Caetano-Silva, M.E., Cilla, A., Bertoldo-Pacheco, M.T., Netto, F.M., Alegría, A., 2017. Evaluation of in vitro iron bioavailability in free form and as whey peptide-iron complexes. J. Food Compos. Anal. https://doi.org/10.1016/j.jfca.2017.03.010.
Caetano-Silva, M.E., Cilla, A., Bertoldo-Pacheco, M.T., Netto, F.M., Alegría, A., 2018. Evaluation of in vitro iron bioavailability in free form and as whey peptide-iron complexes. J. Food Compos. Anal. 68, 95–100. https://doi.org/10.1016/j.jfca.2017.03.010. March 2017.
Caetano-Silva, M.E., Simabuco, F.M., Bezerra, R.M.N., Silva, D.C., Barbosa, E.A., Moreira, D.C., Brand, G.D., Leite, J.R.S.A., Bertoldo-Pacheco, M.T., 2020. Isolation and sequencing of Cu-, Fe-, and Zn-binding whey peptides for potential neuroprotective applications as multitargeted compounds. J. Agric. Food Chem. 68 (44), 12433–12443. https://doi.org/10.1021/acs.jafc.0c03647.
Carlton, D.D., Schug, K.A., 2011. A review on the interrogation of peptide-metal interactions using electrospray ionization-mass spectrometry. Anal. Chim. Acta 686 (1–2), 19–39. https://doi.org/10.1016/j.aca.2010.11.050.
Charley, P.J., Sarkar, B., Stitt, C.F., Saltman, P., 1963. Chelation of iron by sugars. BBA - Biochimica et Biophysica Acta. https://doi.org/10.1016/0006-3002(63)91264-2.
Christides, T., Sharp, P., 2013. Sugars increase non-heme iron bioavailability in human epithelial intestinal and liver cells. PLoS One 8 (12). https://doi.org/10.1371/journal.pone.0083031.
Conrad, M.E., Umbreit, J.N., 2000. Iron absorption and transport - an update. Am. J. Hematol. 64 (4), 287–298. https://doi.org/10.1002/1096-8652(200008)64:4<287::AID-AJH9>3.0.CO;2L.
Cruz-Huerta, E., Maqueda, D.M., de la Hoz, L., Silva, V.S.N., Bertoldo-Pacheco, M.T., Amigo, L., Recio, I., 2016. Identification of iron-binding peptides from whey protein hydrolysates using iron (III)-immobilized metal ion affinity chromatography and reversed phase-HPLC-tandem mass spectrometry. J. Dairy Sci. 99, 77–82. https://doi.org/10.3168/jds.2015-9839.
Do Nascimento da Silva, E., Cadore, S., 2019. Bioavailability assessment of copper, iron, manganese, molybdenum, selenium, and zinc from selenium-enriched lettuce. J. Food Sci. 84 (10), 2840–2846. https://doi.org/10.1111/1750-3841.14785.
DRI, 2006. Institute of Medicine. Dietary reference intakes; the essential guide to nutriente requirements. National Academy Press, Washington (DC), 2006. https://www.nal.usda.gov/sites/default/files/fnic_uploads/DRIEssentialGuideNutReq.pdf .
Eckert, E., Lu, L., Unsworth, L.D., Chen, L., 2016. Biophysical and in vitro absorption studies of iron chelating peptide from barley proteins. J. Funct.Foods 25, 291–301. https://doi.org/10.1016/j.jff.2016.06.011.
Etcheverry, P., Grusak, M.A., Fleige, L.E., 2012. Application of in vitro bioaccessibility and bioavailability methods for calcium, carotenoids, folate, iron, magnesium, polyphenols, zinc, and vitamins B 6, B 12, D, and E. Front. Physiol. 3, 1–22. https://doi.org/10.3389/fphys.2012.00317. AUG(August.
Fabiano, A., Brilli, E., Fogli, S., Beconcini, D., Carpi, S., Tarantino, G., Zambito, Y., 2018. Sucrosomial® iron absorption studied by in vitro and ex-vivo models. Eur. J. Pharmaceut. Sci. 111, 425–431. https://doi.org/10.1016/j.ejps.2017.10.021. June 2017.
Filiponi, M.P., Gaigher, B., Caetano-Silva, M.E., Alvim, I.D., Pacheco, M.T.B., 2019. Microencapsulation performance of Fe-peptide complexes and stability monitoring. Food Res. Int. 125, 108505. https://doi.org/10.1016/j.foodres.2019.108505.
Gharibzahedi, S.M.T., Jafari, S.M., 2017. The importance of minerals in human nutrition: bioavailability, food fortification, processing effects and nanoencapsulation. Trends Food Sci. Technol. 62, 119–132. https://doi.org/10.1016/j.tifs.2017.02.017.
Grancieri, M., Martino, H.S.D., De Mejia, E.G., 2019. Digested total protein and protein fractions from chia seed (Salvia hispanica L.) had high scavenging capacity and inhibited 5-LOX, COX-1-2, and iNOS enzymes. Food Chem. 289, 204–214. https://doi.org/10.1016/j.foodchem.2019.03.036. Epub 2019 Mar 12. PMID: 30955604.
Guzun-Cojocaru, T., Koev, C., Yordanov, M., Karbowiak, T., Cases, E., Cayot, P., 2011. Oxidative stability of oil-in-water emulsions containing iron chelates: transfer of iron from chelates to milk proteins at interface. Food Chem. 125 (2), 326–333. https://doi.org/10.1016/j.foodchem.2010.08.004.
Hagen, S.R., Frost, B., Augustin, J., 1989. Precolumn phenylisothiocyanate derivatization and liquid chromatography of amino acids in food. J. Assoc. Off. Anal. Chem. https://doi.org/10.1093/jaoac/72.6.912.
De Hoz, L., Nunes, V.S., Morgano, M.A., Teresa, M., 2014. Small peptides from enzymatic whey hydrolysates increase dialyzable iron. Int. Dairy J. https://doi.org/10.1016/j.idairyj.2013.12.009.
Hurrell, R., 2002. How to ensure adequate iron absorption from iron-fortified food. Nutr. Rev. 60 (Suppl. 7), S7–S15. https://doi.org/10.1301/002966402320285137.
Hurrell, R., Egli, I., 2019. Fortification of food: principles and practice. In: Means Jr., R. (Ed.), Nutritional Anemia: Scientific Principles, Clinical Practice, and Public Health. Cambridge University Press, Cambridge, pp. 16–30. https://doi.org/10.1017/9781139023993.004.
Kim, S.B., Seo, I.S., Khan, M.A., Ki, K.S., Nam, M.S., Kim, H.S., 2007. Separation of iron-binding protein from whey through enzymatic hydrolysis. Int. Dairy J. 17 (6), 625–631. https://doi.org/10.1016/j.idairyj.2006.09.001.
Li, Y., Jiang, H., Huang, G., 2017. Protein hydrolysates as promoters of non-haem iron absorption. Nutrients. https://doi.org/10.3390/nu9060609.
Lv, Y., Guo, S., Tako, E., Glahn, P., 2014. Hydrolysis of soybean protein improves iron bioavailability by caco-2 cell. J. Food Nutr. Res. 2 (4), 162–166. https://doi.org/10.12691/jfnr-2-4-5.
Ma, Q., Kim, E.-Y., Han, O., 2010. Bioactive dietary polyphenols decrease heme iron absorption by decreasing basolateral iron release in human intestinal caco-2 cells. J. Nutr. 140 (6), 1117–1121. https://doi.org/10.3945/jn.109.117499.
Minekus, M., Alminger, M., Alvito, P., Ballance, S., Bohn, T., Bourlieu, C., Brodkorb, A., 2014. A standardised static in vitro digestion method suitable for food-an international consensus. Food Funct. 5 (6), 1113–1124. https://doi.org/10.1039/c3fo60702j.
Mojica, L., Luna-Vital, D.A., González de Mejía, E., 2017. Characterization of peptides rom common bean protein isolates and their potential to inhibit markers of type-2 M. Grancieri, et al. Food Chemistry 289 (2019) 204–214 213diabetes, hypertension and oxidative stress. J. Sci. Food Agric. 97 (8), 2401–2410. https://doi.org/10.1002/jsfa.8053.
Morgano, M.A., Queiroz, S.C.N., Ferreira, M.M.C., 1999. Determinação dos teores de minerais em sucos de frutas por espectrometria de emissão óptica em plasma indutivamente acoplado (ICP-OES). Disponível em. Food Science and Technology, pp. 344–348. https://doi.org/10.1590/S0101-20611999000300009. Epub 21 Ago 2000. ISSN 1678-457X. 10.1590/S0101-20611999000300009.
Morris, G.M., Huey, R., Lindstrom, W., Sanner, M.F., Belew, R.K., Goodsell, D.S., Olson, A.J., 2009. AutoDock4 andAutoDockTools4: automated docking with selective receptor flexibility. J. Comput. Chem. 30, 2785–2791.
Muñoz, E.B., Luna-Vital, D.A., Fornasini, M.E., Baldeón, M., Gonzalez de Mejia, E., 2018. Gamma-conglutin peptides from Andean lupin legume (Lupinus mutabilis Sweet) enhanced glucose uptake and reduced gluconeogenesis in vitro. J. Funct. Foods 45, 339–347. https://doi.org/10.1016/j.jff.2018.04.021.
Nelson, D.L., Cox, M.M., 2016. Protein Function. In: Lehninger Principles of Biochemistry. W.H. Freeman Publishers, New York, NY, pp. 151–182 (Chapter 5). https://macmillanlearning.com/Lehninger7e.
Nielsen, P.M., Petersen, D., Dambmann, C., 2001. Improved method for determining food protein degree of hydrolysis. J. Chem. Toxicol. 66 (5), 642–646.
Oleg, T., Arthur, O.J., 2010. AutoDock Vina: improving the speed and accuracy of docking with a new scoring function, efficient optimization, and multithreading. J. Comput. Chem. 31, 455–461.
Ou, K., Liu, Y., Zhang, L., Yang, X., Huang, Z., Nout, M.J.R., Liang, J., 2010. Effect of neutrase, alcalase, and papain hydrolysis of whey protein concentrates on iron uptake by Caco-2 cells. J. Agric. Food Chem. 58 (8), 4894–4900. https://doi.org/10.1021/jf100055y.
Price, W.J., Roos, J.T.H., 1969. Analysis of fruit juice by atomic absorption spectrophotometry I.—the determination of iron and tin in canned juice. J. Sci. Food Agric. https://doi.org/10.1002/jsfa.2740200717.
Ren, Z.Y., Huang, G.R., Jiang, J.X., Chen, W.W., 2011. Preparation and characteristic of iron-binding peptides from shrimp processing discards hydrolysates. Adv. J. Food Sci. Technol. 3 (5), 348–354.
Salovaara, S., Sandberg, A.S., Andlid, T., 2002. Organic acids influence iron uptake in the human epithelial cell line Caco-2. J. Agric. Food Chem. 50 (21), 6233–6238. https://doi.org/10.1021/jf0203040.
Scheers, N.M., Almgren, A.B., Sandberg, A.S., 2014. Proposing a Caco-2/HepG2 cell model for in vitro iron absorption studies. JNB (J. Nutr. Biochem.) 25 (7), 710–715. https://doi.org/10.1016/j.jnutbio.2014.02.013.
Shubham, K., Anukiruthika, T., Dutta, S., Kashyap, A.V., Moses, J.A., Anandharamakrishnan, C., 2020. Iron deficiency anemia: a comprehensive review on iron absorption, bioavailability and emerging food fortification approaches. Trends Food Sci. Technol. 99 (January), 58–75. https://doi.org/10.1016/j.tifs.2020.02.021.
Sugiarto, M., Ye, A., Taylor, M.W., Singh, H., 2010. Milk protein-iron complexes: inhibition of lipid oxidation in an emulsion. Dairy Sci. Technol. 90 (1), 87–98. https://doi.org/10.1051/dst/2009053.
Sun, X., Sarteshnizi, R.A., Boachie, R.T., Okagu, O.D., Abioye, R.O., Neves, R.P., Udenigwe, C.C., 2020. Peptide-mineral complexes: understanding their chemical interactions, bioavailability, and potential application in mitigating micronutrient deficiency. Foods 9 (10). https://doi.org/10.3390/foods9101402.
Szarfarc, S.C., 2010. Políticas públicas para o controle da anemia ferropriva. Rev. Bras. Hematol. Hemoter. 32 (55 11) https://doi.org/10.1590/S1516-84842010005000065, 02–08.

Trijatmiko, K.R., Duenãs, C., Tsakirpaloglou, N., Torrizo, L., Arines, F.M., Adeva, C., Slamet-Loedin, I.H., 2016. Biofortified indica rice attains iron and zinc nutrition dietary targets in the field. Sci. Rep. 6, 1–13. https://doi.org/10.1038/srep19792. September 2015.

Ueno, H.M., Urazono, H., Kobayashi, T., 2014. Serum albumin forms a lactoferrin-like soluble iron-binding complex in presence of hydrogen carbonate ions. Food Chem. 145, 90–94. https://doi.org/10.1016/j.foodchem.2013.07.143.

Wang, X., Ai, T., Meng, X.L., Zhou, J., Mao, X.Y., 2014. In vitro iron absorption of α-lactalbumin hydrolysate-iron and β-lactoglobulin hydrolysate-iron complexes. J. Dairy Sci. 97 (5), 2559–2566. https://doi.org/10.3168/jds.2013-7461.

White, J.A., Hart, R.J., Fry, J.C., 1986. An evaluation of the Waters Pico-Tag system for the amino-acid analysis of food materials. J. Automat. Chem. https://doi.org/10.1155/S1463924686000330.

WHO, 2016. Guideline Daily Iron. Daily Iron Supplementation in Infants and Children. Available from: https://www.ncbi.nlm.nih.gov/books/NBK362032/.

Wu, H., Liu, Z., Zhao, Y., Zeng, M., 2012. Enzymatic preparation and characterization of iron-chelating peptides from anchovy (Engraulis japonicus) muscle protein. Food Res. Int. https://doi.org/10.1016/j.foodres.2012.04.013.

Xu, Z., Sun, W., Li, Y., Ling, S., Zhao, C., Zhong, G., Li, Y., 2017. The regulation of iron metabolism by hepcidin contributes to unloading-induced bone loss. Bone 94, 152–161. https://doi.org/10.1016/j.bone.2016.09.023.

Zhang, D.L., Ghosh, M.C., Rouault, T.A., 2014. The physiological functions of iron regulatory proteins in iron homeostasis - an update. Front. Pharmacol. 5, 1–12. https://doi.org/10.3389/fphar.2014.00124. *JUN*(June).

Zhou, J., Wang, X., Ai, T., Cheng, X., Guo, H.Y., Teng, G.X., Mao, X.Y., 2012. Preparation and characterization of β-lactoglobulin hydrolysate-iron complexes. J. Dairy Sci. 95 (8), 4230–4236. https://doi.org/10.3168/jds.2011-5282.

Zhu, L., Glahn, R.P., Nelson, D., Miller, D.D., 2009. Comparing soluble ferric pyrophosphate to common iron salts and chelates as sources of bioavailable iron in a Caco-2 cell culture model. J. Agric. Food Chem. 57 (11), 5014–5019. https://doi.org/10.1021/jf900328t.